Interband coupling and nonmagnetic interband scattering in $\pm s$ superconductors

V. G. Kogan[1,*] and R. Prozorov[1,2,†]
[1]*Ames Laboratory, Ames, Iowa 50011, USA*
[2]*Department of Physics & Astronomy, Iowa State University, Ames, Iowa 50011, USA*
(Received 4 April 2016; revised manuscript received 22 May 2016; published 17 June 2016)

A two-band model with repulsive interband coupling and interband *potential* scattering is considered to elucidate their effects on material properties. In agreement with previous work, we find that the bands' order parameters $\Delta_{1,2}$ differ, and the larger is at the band with a smaller normal density of states (DOS), $N_{n2} < N_{n1}$. However, the bands' energy gaps, as determined by the energy dependence of the DOS, are equal due to scattering. For each temperature, the gaps become zero at a certain critical interband scattering rate; i.e., for strong enough scattering the model material becomes gapless. In the gapless state, the DOS at band 2 is close to the normal state value, whereas at band 1 it has a V shape with nonzero minimum. When the normal bands DOS are mismatched, $N_{n1} \neq N_{n2}$, the critical temperature T_c is suppressed even in the absence of interband scattering, $T_c(N_{n1})$ has a domelike shape. With increasing interband scattering, the London penetration depth at low temperatures evolves from being exponentially flat to a power law and even to near linear behavior in the gapless state, the latter being easily misinterpreted as caused by order parameter nodes.

DOI: 10.1103/PhysRevB.93.224515

I. INTRODUCTION

It is by now an accepted view that the interband scattering in two-band $\pm s$ superconductors suppresses the critical temperature, i.e., has a pair-breaking effect; see, e.g., Refs. [1–7]. The interband coupling and interband scattering are of a particular interest because both are thought to play a special role in the physics of two-band materials in general [2–6,8–10] and of the extensive family of Fe-based compounds, in particular [11–13]. A theoretical description of the multiband situation requires a multitude of parameters to represent couplings along with intra- and interband scatterings [14]. For this reason, we focus here on a model with only interband coupling (repulsive, to have $\pm s$ order parameter) and with a nonmagnetic interband scattering. Although such a model cannot be applied to real materials, it allows one to single out physical consequences of the interband scattering which may help in data interpretation.

II. APPROACH

Our approach is based on the quasiclassical version of the *weak-coupling* BCS theory for anisotropic Fermi surfaces and order parameters [15]. This theory is formulated in terms of the Eilenberger Green's functions f, f^+, and g (averaged over the energy Gor'kov's functions):

$$\mathbf{v}\cdot\mathbf{\Pi} f = 2\Delta g - 2\omega f + I, \tag{1}$$

$$g^2 = 1 - ff^+. \tag{2}$$

Here $\boldsymbol{v}$ is the Fermi velocity and $\mathbf{\Pi} = \nabla + 2\pi i\mathbf{A}/\phi_0$, with the vector potential $\boldsymbol{A}$ and the flux quantum ϕ_0. $\Delta(\boldsymbol{k})$ is the order parameter and $\boldsymbol{k}$ is the Fermi momentum. Matsubara frequencies are $\omega = \pi T(2l+1)$ with an integer l; throughout this text ω and T are in energy units, $\hbar = k_B = 1$. The equation for f^+ is obtained from Eq. (1) by taking the complex conjugate and replacing $\mathbf{v} \to -\mathbf{v}$.

The scattering term I is given by the integral over the full Fermi surface:

$$I(\boldsymbol{k}) = \int d^2\boldsymbol{q}\,\rho(\boldsymbol{q})\,W(\boldsymbol{k},\boldsymbol{q})[g(\boldsymbol{k})f(\boldsymbol{q}) - f(\boldsymbol{k})g(\boldsymbol{q})]; \tag{3}$$

$W(\boldsymbol{k},\boldsymbol{q})$ is the Born probability of scattering from $\boldsymbol{q}$ to $\boldsymbol{k}$. The DOS $\rho(\boldsymbol{q})$ is normalized: $\int d^2\boldsymbol{q}\,\rho(\boldsymbol{q}) = 1$.

We use approximation of the scattering time τ:

$$\int d^2\boldsymbol{q}\,\rho(\boldsymbol{q})\,W(\boldsymbol{k},\boldsymbol{q})\,\Phi(\boldsymbol{q}) = \langle\Phi\rangle/\tau\,; \tag{4}$$

$\langle\cdots\rangle$ stands for the average over the Fermi surface. Clearly, the approximation amounts to the scattering probability $W = 1/\tau$ being constant for any $\boldsymbol{k}$ and $\boldsymbol{q}$. However, for two well-separated Fermi surface sheets, the probabilities of intraband scatterings may differ from each other and from processes involving $\boldsymbol{k}$ and $\boldsymbol{q}$ from different bands. The effects of the inter- and intraband scattering upon various properties of the system are different. Hence, Eq. (4) is replaced with [16]

$$\int d^2\boldsymbol{q}_\nu\,\rho(\boldsymbol{q}_\nu)\,W(\boldsymbol{k}_\mu,\boldsymbol{q}_\nu)\,\Phi(\boldsymbol{q}_\nu) = n_\nu\langle\Phi\rangle_\nu/\tau_{\mu\nu}. \tag{5}$$

Here $\nu,\mu = 1,2$ are band indices; $\langle\cdots\rangle_\nu$ denotes averaging over the ν band, and $n_\nu = \int d^2\boldsymbol{q}_\nu\,\rho(\boldsymbol{q}_\nu) = N_\nu/N(0)$ are relative densities of states: $n_1 + n_2 = 1$.

In the absence of magnetic fields, all functions involved are real, $f^+ = f$, and we have

$$0 = 2\Delta g - 2\omega f + I, \quad 1 = g^2 + f^2. \tag{6}$$

We assume the order parameter takes constant values Δ_1 and Δ_2 at the two bands. Writing Eq. (6) for $\boldsymbol{k}$ in the first band, we have

$$0 = 2\Delta_1 g_1 - 2\omega f_1 + \frac{n_1}{\tau_{11}}(g_1\langle f\rangle_1 - f_1\langle g\rangle_1) + \frac{n_2}{\tau_{12}}(g_1\langle f\rangle_2 - f_1\langle g\rangle_2). \tag{7}$$

*kogan@ameslab.gov
†Corresponding author: prozorov@ameslab.gov

For a uniform sample in zero field and with $\boldsymbol{k}$-independent Δ's in each band, the functions f,g are $\boldsymbol{k}$ independent, i.e., $\langle f\rangle_\nu = f_\nu$ and $\langle g\rangle_\nu = g_\nu$:

$$0 = \Delta_1 g_1 - \omega f_1 + n_2(g_1 f_2 - f_1 g_2)/2\tau_{12}. \tag{8}$$

The equation for the second band differs from this by the replacement $1 \leftrightarrow 2$. The fact that τ_{11} and τ_{22} do not enter the system (8) is similar to the case of one-band isotropic material for which nonmagnetic scattering has no effect upon T_c (the Anderson theorem). It is the inter-band scattering that makes the difference in the two-band case, a fact stressed already in early work [3,4]. For brevity, we use the notation $\tau_{12} = \tau$ unless τ_{11},τ_{22} should be explicitly distinguished from τ_{12}.

Equations (8) are complemented with normalizations,

$$g_\nu^2 + f_\nu^2 = 1, \quad \nu = 1,2, \tag{9}$$

and by the self-consistency equation for the order parameter:

$$\Delta(\boldsymbol{k}) = 2\pi T N_n \sum_{\omega>0}^{\omega_D} \langle V(\boldsymbol{k},\boldsymbol{k}')f(\boldsymbol{k}',\omega)\rangle_{\boldsymbol{k}'}. \tag{10}$$

Here, N_n is the total density of states at the Fermi level per spin in the normal phase; ω_D is the Debye frequency (or the energy of whatever "glue boson"). Within the weak-coupling scheme, the coupling potential V responsible for superconductivity is a 2×2 matrix of constants $V_{\nu\mu}$. The self-consistency equation (10) takes the form [17]

$$\Delta_\nu = 2\pi T \sum_{\mu,\omega}^{\omega_D} n_\mu \lambda_{\nu\mu} f_\mu, \quad \nu = 1,2; \tag{11}$$

$\lambda_{\nu\mu} = N_n V_{\nu\mu}$ are dimensionless coupling constants.

To separate effects of the interband coupling and scattering from other possible multiband consequences, we set $\lambda_{11} = \lambda_{22} = 0$, whereas λ_{12} (denoted as λ in the text below) is assumed *negative*. This leads to the order parameters Δ_1 and Δ_2 having opposite signs [3,11,18], i.e., to $\pm s$ superconductivity, which presumably exists in many Fe-based materials. Hence, we have

$$\Delta_1 = 2\pi T\lambda n_2 \sum_{\omega}^{\omega_D} f_2, \quad \Delta_2 = 2\pi T\lambda n_1 \sum_{\omega}^{\omega_D} f_1. \tag{12}$$

Hereafter, we take Δ_1 as being positive. Since $\lambda < 0$, these equations imply negative Δ_2. Accordingly, in the current-free phase $f_1 > 0$ and $f_2 < 0$; in particular, this prescribes the sign of the square root if the normalization (9) is used to express f's: $f_1 = \sqrt{1-g_1^2}$, $f_2 = -\sqrt{1-g_2^2}$.

As in original work by Eilenberger [15], the energy functional Ω can be constructed so that Eqs. (8) and (12) follow as extremum conditions relative to variations of f_ν and Δ_ν:

$$\frac{\Omega}{N(0)} = \frac{2\Delta_1\Delta_2}{\lambda} - 2\pi T \sum_{\omega} \left\{ \sum_{\nu} 2n_\nu[\Delta_\nu f_\nu + \omega(g_\nu - 1)] + \frac{n_1 n_2}{\tau}(f_1 f_2 + g_1 g_2 - 1)\right\}. \tag{13}$$

Here, g_ν are abbreviations for $\sqrt{1-f_\nu^2}$, and $\delta g_\nu = -(f_\nu/g_\nu)\,\delta f_\nu$. If f_ν are solutions of Eqs. (8) and Δ_ν satisfy the self-consistency equations (12), Ω coincides with the condensation energy $F_S - F_N$ and can be used to study thermodynamic properties of a uniform two-band system.

Equations (8), (12), and (13) form the basis of our approach. Only in a few simple situations can the results be obtained in a closed form. In most cases, the analytic approach, if at all possible, is too cumbersome, and we resort to numerical solutions which are relatively straightforward with available tools such as MATHEMATICA or MATLAB.

III. CLEAN CASE

It is instructive to begin with the clean limit, $\tau \to \infty$, although it has been considered in literature [19–21]. In this case, we have from Eqs. (8) and (9)

$$f_\nu = \Delta_\nu/\beta_\nu, \quad g_\nu = \omega/\beta_\nu, \quad \beta_\nu^2 = \omega^2 + \Delta_\nu^2. \tag{14}$$

At $T = 0$, the sums in Eqs. (12) are evaluated by replacing $2\pi T\sum_\omega \to \int_0^{\omega_D} d\omega$, which gives

$$\Delta_1 = \lambda n_2 \Delta_2 \ln\frac{2\omega_D}{|\Delta_2|}, \quad \Delta_2 = \lambda n_1 \Delta_1 \ln\frac{2\omega_D}{|\Delta_1|}. \tag{15}$$

Expressing the logarithmic factors and subtracting the results, one obtains for the ratio $R = |\Delta_2/\Delta_1|$

$$|\lambda| \ln R = \frac{R}{n_1} - \frac{1}{n_2 R}. \tag{16}$$

Given $n_{1,2}$ and λ, this can be solved numerically for R. For example, for $\lambda = -0.6$ and $n_1 = 0.6, n_2 = 0.4$, we obtain $R \approx 1.27$, whereas for $n_1 = 0.4, n_2 = 0.6$ we have $R \approx 0.79$. Hence, the order parameter value is larger at the band with a smaller DOS [22].

For a given R, Eqs. (15) yield

$$|\Delta_1| = 2\omega_D \exp\left(-\frac{R}{n_1|\lambda|}\right), \quad |\Delta_2| = 2\omega_D \exp\left(-\frac{1}{n_2|\lambda|R}\right). \tag{17}$$

Hence, $n_1|\lambda|/R$ and $n_2|\lambda|R$ are effective coupling constants for the first and second bands, respectively.

To evaluate the condensation energy at $T = 0$, consider the sum that enters the energy (13):

$$4\pi T \sum_{\omega>0}^{\omega_D} n_1\left[\frac{\Delta_1^2}{\beta_1} + \omega\left(\frac{\omega}{\beta_1} - 1\right)\right] = 2n_1\int_0^{\omega_D}(\beta_1 - \omega)d\omega = n_1\left(\frac{\Delta_1^2}{2} + \Delta_1^2 \ln\frac{2\omega_D}{|\Delta_1|}\right) = \frac{n_1\Delta_1^2}{2} + \frac{\Delta_1\Delta_2}{\lambda}, \tag{18}$$

where Eqs. (15) have been used. Hence, we obtain

$$(F_S - F_N)_{T=0} = -N_n\frac{n_1\Delta_1^2 + n_2\Delta_2^2}{2} = -N_n\frac{\langle\Delta^2\rangle}{2}. \tag{19}$$

Recall that in isotropic one-band superconductors this energy is $-N_n\Delta^2/2$.

As $T \to T_{c0}(n_1)$ (the critical temperature of a clean material for a given n_1) $f_\nu = \Delta_\nu/\omega$ and the sums in Eqs. (12) can be

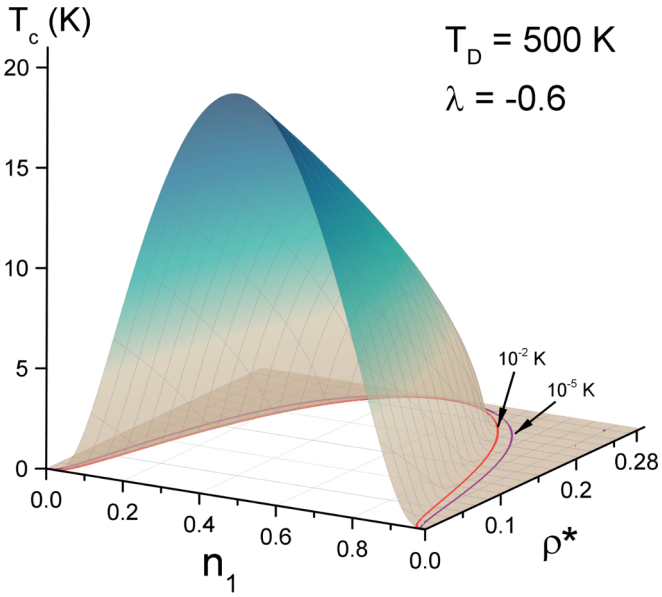

FIG. 1. $T_c(n_1,\rho^*)$ for $T_D = 500$ K, $\lambda = -0.6$. The line at the dome base gives the value of the rate $\rho^* = 1/2\pi T_{c0}(0.5)\tau$ at which the $T_c = 5\times 10^{-4} T_{c0}(0.5) \approx 0.01$ K, where the superconductivity is practically destroyed. For $n_1 = 0.5$, $\rho^*_{\rm cr} = e^{-\gamma}/2 = 0.28$ and the critical rate is $1/\tau_{\rm cr} = \Delta_0(0)$; $\Delta_0(0)$ is the order parameter of clean material with $n_1 = n_2$ at $T = 0$. It is argued in the next subsection that in fact $T_c \neq 0$ at the rest of the shaded picture base, but it is extremely small there and becomes exactly zero at the base edges.

evaluated:

$$\frac{\Delta_1}{\Delta_2} = \lambda n_2 \ln\frac{2\omega_D e^\gamma}{\pi T_{c0}}, \quad \frac{\Delta_2}{\Delta_1} = \lambda n_1 \ln\frac{2\omega_D e^\gamma}{\pi T_{c0}}. \tag{20}$$

Multiplying these, one extracts the logarithmic factor and the critical temperature:

$$\pi e^{-\gamma} T_{c0} = 2\omega_D \exp(-1/\tilde\lambda), \quad \tilde\lambda = |\lambda|\sqrt{n_1 n_2}. \tag{21}$$

Hence,

$$\tilde\lambda = |\lambda|\sqrt{n_1 n_2} \tag{22}$$

plays the role of the overall coupling constant.

It is worth noting that, for a fixed coupling λ, the critical temperature T_{c0} as a function of relative DOS n_1 has a domelike shape; see Fig. 1. Thus within the model of exclusively interband coupling, a mismatch of bands' DOS suppresses T_c even in the absence of scattering. Qualitatively, this happens because for $n_1 \neq n_2$ the number of unpaired carriers is proportional to $|n_1 - n_2|$.

Turning back to Eqs. (20) one finds the ratio [21]

$$R(T_{c0}) = \left|\frac{\Delta_2}{\Delta_1}\right| = \sqrt{\frac{n_1}{n_2}}. \tag{23}$$

Compare this with Eq. (16) for $T = 0$ to see that in fact Δ_2/Δ_1 depends on T.

Next, we calculate Δ_ν with the help of the self-consistency system (12). Note first that near T_{c0}, $\beta_\nu \approx \omega(1 + \Delta_\nu^2/2\omega^2)$ and, therefore,

$$f_\nu = \frac{\Delta_\nu}{\omega} - \frac{\Delta_\nu^3}{2\omega^3} + \mathcal{O}(\delta t)^{5/2}; \tag{24}$$

here $\Delta \propto (\delta t)^{1/2}$, $\delta t = 1 - T/T_{c0}$. The sums in Eq. (12) are

$$\sum_0^{\omega_D} \frac{2\pi T}{\omega} = \ln\frac{2\omega_D e^\gamma}{\pi T_{c0}} = \frac{1}{\tilde\lambda} + \delta t, \quad \sum_0^{\infty} \frac{2\pi T}{\omega^3} = \frac{7\zeta(3)}{4\pi^2 T_{c0}^2} \tag{25}$$

and we obtain

$$\begin{aligned}\Delta_1 &= \lambda n_2 \Delta_2 \left(\frac{1}{\tilde\lambda} + \delta t - \frac{7\zeta(3)}{8\pi^2 T_{c0}^2}\Delta_2^2\right),\\ \Delta_2 &= \lambda n_1 \Delta_1 \left(\frac{1}{\tilde\lambda} + \delta t - \frac{7\zeta(3)}{8\pi^2 T_{c0}^2}\Delta_1^2\right).\end{aligned} \tag{26}$$

This system should be solved keeping terms of order not higher than $(\delta t)^{3/2}$. One substitutes Δ_2 from the second equation to the first to obtain [21]

$$\Delta_1^2 = \frac{16\pi^2 T_{c0}^2 \delta t}{7\zeta(3)} n_2, \quad \Delta_2^2 = \frac{16\pi^2 T_{c0}^2 \delta t}{7\zeta(3)} n_1. \tag{27}$$

Thus, the gaps' ratio *near* T_{c0} is the same as at T_{c0} [23].

The energy near T_{c0} should be evaluated including terms of the order $(\delta t)^2$. In particular,

$$g_\nu = 1 - \frac{f_\nu^2}{2} - \frac{f_\nu^4}{8} = 1 - \frac{\Delta_\nu^2}{2\omega^2} + \frac{3\Delta_\nu^4}{8\omega^4}. \tag{28}$$

Straightforward algebra shows that terms of the order $\Delta^2 \sim \delta t$ cancel out and the rest give

$$F_S - F_N = -N(0) n_1 n_2 \frac{16\pi^2 T_{c0}^2}{7\zeta(3)}\left(1 - \frac{T}{T_{c0}}\right)^2. \tag{29}$$

Thus, the specific heat jump is [17,24]

$$\left.\frac{C_S - C_N}{C_N}\right|_{T_c} = \frac{48}{7\zeta(3)} n_1 n_2. \tag{30}$$

The maximum value of this ratio $12/7\zeta(3) = 1.43$ is achieved if $n_1 = n_2 = 1/2$.

IV. EFFECTS OF SCATTERING

In general, in the presence of the interband scattering, the system of Eqs. (8) and (12) can be solved only numerically. Near T_c, however, Eqs. (8) can be linearized and f_ν are readily expressed in terms of Δ_ν:

$$\begin{aligned} f_\nu &= \frac{\Delta_\nu}{\omega'} + \frac{\langle\Delta\rangle}{2\omega\omega'\tau},\\ \langle\Delta\rangle &= n_1\Delta_1 + n_2\Delta_2, \quad \omega' = \omega + 1/2\tau.\end{aligned} \tag{31}$$

Substituting this in the self-consistency system (12), one obtains a system of linear homogeneous equations for $\Delta_{1,2}$, which has nontrivial solutions only if its determinant is zero. This gives an implicit equation for T_c:

$$0 = 1 - 2n_1 n_2 \lambda B - n_1 n_2 \lambda^2 A(A + B), \tag{32}$$

$$\begin{aligned} A &= \ln\frac{\omega_D}{2\pi T_c} - \psi\left(\frac{\rho_c + 1}{2}\right)\\ &= \frac{1}{\tilde\lambda} + \ln\frac{T_{c0}}{T_c} - \psi\left(\frac{\rho_c + 1}{2}\right) + \psi\left(\frac{1}{2}\right),\end{aligned} \tag{33}$$

$$B = \psi\left(\frac{\rho_c + 1}{2}\right) - \psi\left(\frac{1}{2}\right), \quad \rho_c = \frac{1}{2\pi T_c \tau}. \tag{34}$$

If $n_1 = n_2 = 1/2$ and $\tilde{\lambda} = |\lambda|/2$, Eq. (32) reduces to a quadratic equation for $\ln(T_{c0}/T_c)$. This gives

$$\ln\frac{T_{c0}}{T_c} = \psi\left(\frac{\rho_c+1}{2}\right) - \psi\left(\frac{1}{2}\right), \tag{35}$$

which coincides with the equation for T_c suppression by impurities for a d-wave one-band superconductor, or generally, for order parameters with zero Fermi surface averages [5,25,26]. In particular, this means that for this case T_c becomes zero at a critical value of interband scattering time $\tau = 1/\Delta_0(0)$, one-half of the Abrikosov-Gor'kov's value for the effect of magnetic impurities upon one-band s-wave isotropic superconductors [27,28].

A. $T_c(n_1,\tau)$

Consider now how the critical temperature changes with changing n_1 and the scattering rate $1/\tau$. Solving Eqs. (32)–(34), we have to take into account that the clean case T_{c0} depends on n_1. To proceed with numerical calculations in this particular problem, we normalize the temperature:

$$t^* = \frac{T}{T_{c0}(0.5)}, \quad t_c^* = \frac{T_c}{T_{c0}(0.5)}. \tag{36}$$

Here, $T_c(n_1,\tau)$ is the actual critical temperature and $T_{c0}(0.5)$ is the maximum possible critical temperature of the clean material reached at $n_1 = 0.5$.

Also, we introduce the scattering parameters

$$\rho^* = \frac{1}{2\pi\tau T_{c0}(0.5)}, \quad \rho_c = \frac{1}{2\pi\tau T_c} = \frac{\rho^*}{t_c^*} \tag{37}$$

so that ρ^* is independent of n_1. Next, we transform the logarithmic term in A of Eq. (33):

$$A = \frac{2}{|\lambda|} - \ln t_c^* + \psi\left(\frac{1}{2}\right) - \psi\left(\frac{\rho^*/t_c^*+1}{2}\right). \tag{38}$$

One should also replace $\rho_c \to \rho^*/t_c^*$ in B of Eq. (34). The numerical solutions of Eq. (32) for the critical temperature are given in Fig. 1.

Hence, not only is T_c suppressed by the interband scattering for a fixed n_1, but the DOS asymmetry $(n_1 - 0.5)$ also causes T_c suppression. One thus concludes that, for negative interband coupling λ, there are two mechanisms for the T_c suppression (pair breaking): the interband *potential* scattering and the mismatch of the densities of states of two bands. In particular, in the presence of interband scattering, the interval of DOS mismatch, in which the superconductivity exists, shrinks.

B. The critical scattering rate

To obtain the rate ρ_{cr}^* at which $T_c = 0$ for a fixed n_1, we turn to Eqs. (32)–(34) for T_c. As $T_c \to 0$, $\rho_c \to \infty$, and one obtains in this limit

$$A = -\ln\frac{\omega_D}{\pi T_{c0}(n_1)\rho_{cr}^*}, \quad B = \ln\frac{2e^\gamma\rho_{cr}^*}{t_c^*}. \tag{39}$$

Substitute these in Eq. (32) for T_c and select terms with divergent $\ln t_c^*$:

$$n_1 n_2\lambda\left(2 + \lambda\ln\frac{\omega_D}{\pi T_{c0}(n_1)\rho_{cr}^*}\right)\ln t_c^*. \tag{40}$$

The rest of the terms are not divergent. For this equation to make sense, the coefficient in front of $\ln t_c^*$ must be zero. With the help of Eq. (21) for $T_{c0}(n_1)$, one obtains

$$\rho_{cr}^* = 1/2e^\gamma = 0.2808. \tag{41}$$

We note that this value does not depend on n_1 so that $T_c = 0$ along the edge $\rho^* = 0.28$ of the shaded area of the dome basis plane of Fig. 1.

One can also ask, at what n_1 does the critical temperature become zero if the scattering rate is fixed at $\rho^* < 0.28$? Clearly, the same argument leads to Eq. (40) with ρ_{cr}^* replaced with the rate ρ^*. Now, however, the term in parentheses in this equation is not zero; therefore, the critical values of n_1 are 1 or 0. Thus, in the whole shaded area of the dome basis plane of Fig. 1, T_c is finite, though extremely small; see the two representative contours of $T_c = 10^{-2}$ K and 10^{-5} K. The presence of long and extremely low T_c tails is a formal consequence of interband scattering for $n_1 \neq n_2$.

C. $T_c(\tau)$ for a fixed n_1

In the rest of the text, we consider system properties for a fixed normal state DOS n_1. It is more convenient to employ reduced temperatures

$$t = \frac{T}{T_{c0}(n_1)}, \quad t_c = \frac{T_c}{T_{c0}(n_1)}, \tag{42}$$

and the scattering parameters

$$\rho_0 = \frac{1}{2\pi\tau T_{c0}(n_1)}, \quad \rho_c = \frac{1}{2\pi\tau T_c} = \frac{\rho_0}{t_c}. \tag{43}$$

Figure 2 shows the $T_c(\rho_0)$ for $n_1 = 0.5$ and 0.7 obtained by solving Eqs. (32)–(34). Note that, for $n_1 = n_2$, the critical value of ρ_0 is $e^{-\gamma}/2 \approx 0.28$. Note also that ρ_0 characterizes the scattering along with the DOS mismatch. For this reason, the critical value $\rho_{0,cr}$ for $n_1 = 0.7$ exceeds 0.28 since $T_{c0}(0.7) < T_{c0}(0.5)$.

If $\lambda_{12} > 0$, T_c is only weakly reduced by the interband scattering. This behavior is qualitatively similar to the one-band s-wave materials with anisotropic Fermi surfaces; see,

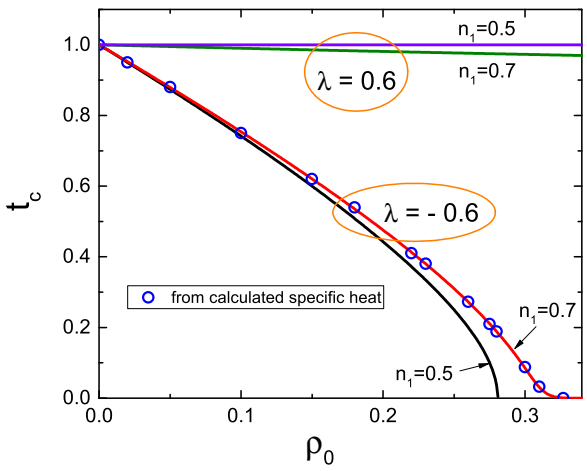

FIG. 2. $t_c = T_c/T_{c0}$ vs ρ_0 according to Eqs. (32)–(34). Lower curves are for $\lambda = -0.6$; the dots are obtained by independent calculation of the specific heat jumps. The upper curves are for positive (attractive) interband coupling constant $\lambda = 0.6$.

e.g., Refs. [14,17,24]. Note that the T_c suppression is stronger for larger differences of n_1 and n_2.

D. Order parameters

Except in the trivial one-band isotropic case for which Δ coincides with the gap in electronic spectrum, the order parameter *per se* is not a measurable quantity. Formally, however, one needs Δ_ν to evaluate observables such as DOS, the specific heat, or the penetration depth.

To find $\Delta_\nu(T)$ we have to solve the system of Eqs. (8) and (12). Near T_c one can do this analytically and verify that $\Delta_\nu \propto \sqrt{T_c - T}$. We, however, resort to numerical evaluation for arbitrary temperatures and use the analytical limits to verify the results. We use dimensionless variables,

$$\delta_\nu = \frac{\Delta_\nu}{2\pi T_{c0}}, \quad t = \frac{T}{T_{c0}}, \quad \rho_0 = \frac{1}{2\pi T_{c0}\tau}. \tag{44}$$

The first of Eqs. (8) for f_1, f_2 takes the form

$$\delta_1 g_1 - f_1 t(l + 1/2) + \frac{n_2\rho_0}{2}(f_2 g_1 - f_1 g_2) = 0, \tag{45}$$

where l is the Matsubara integer and $g_\nu = \sqrt{1 - f_\nu^2}$. The second equation is obtained by replacing $1 \leftrightarrow 2$.

The first self-consistency Eq. (12) is (see Appendix A)

$$\frac{\sqrt{n_1}\delta_1 + \sqrt{n_2}\delta_2}{\tilde{\lambda}\sqrt{n_2}} - \delta_2 \ln t = \sum_{i=0}^{\infty}\left(\frac{\delta_2}{l + 1/2} - t\, f_2\right). \tag{46}$$

The second is obtained by replacing $1 \leftrightarrow 2$. Solving the system of four Eqs. (45) and (46) numerically, we obtain $\Delta_\nu(T)$. Examples are shown in Fig. 3. We note that, as in the clean case, the order parameter is larger at the band with smaller DOS at all Ts and for all ρ_0. One sees that near T_c, $\Delta_\nu \propto \sqrt{\delta t}$ as it should. This is shown analytically for $n_1 = n_2$ in Appendix B.

E. Density of states

As long as $\Delta_\nu(T)$ are known, one can evaluate DOS N_ν as functions of energy ϵ at any fixed T:

$$N_\nu(T,\epsilon) = n_\nu N_n \,\mathrm{Re}[g_\nu(\omega \to i\epsilon)]. \tag{47}$$

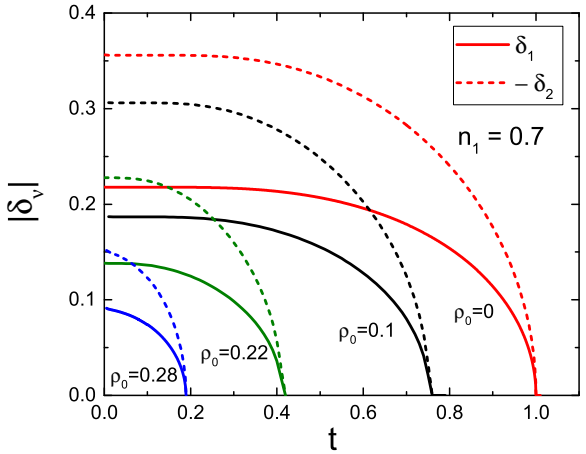

FIG. 3. $|\Delta_\nu|/2\pi T_c$ vs $t = T/T_{c0}$ for $\lambda = -0.6$, $n_1 = 0.7$, and a few values of $\rho_0 = 1/2\pi T_{c0}\tau$.

To this end, one can replace $\omega \to i\epsilon$ already in Eqs. (8):

$$0 = \Delta_1 g_1 - i\,\epsilon f_1 + n_2(g_1 f_2 - f_1 g_2)/2\tau,$$
$$f_1 = \sqrt{1 - g_1^2}, \quad f_2 = -\sqrt{1 - g_2^2}. \tag{48}$$

The dimensionless system of equations for g_ν becomes

$$0 = \delta_1 g_1 - i\,\varepsilon f_1 + \frac{n_2\rho_0}{2}(g_1 f_2 - g_2 f_1), \quad \varepsilon = \frac{\epsilon}{2\pi T_{c0}} \tag{49}$$

(the second equation has $1 \leftrightarrow 2$). The total DOS is $N(T,\epsilon) = N_1(T,\epsilon) + N_2(T,\epsilon)$. Note that DOS depends on T via $\Delta_\nu(T)$. Figure 4 shows examples of $N(T,\epsilon)$. The situation is similar to the Abrikosov-Gor'kov pair-breaking by magnetic impurities

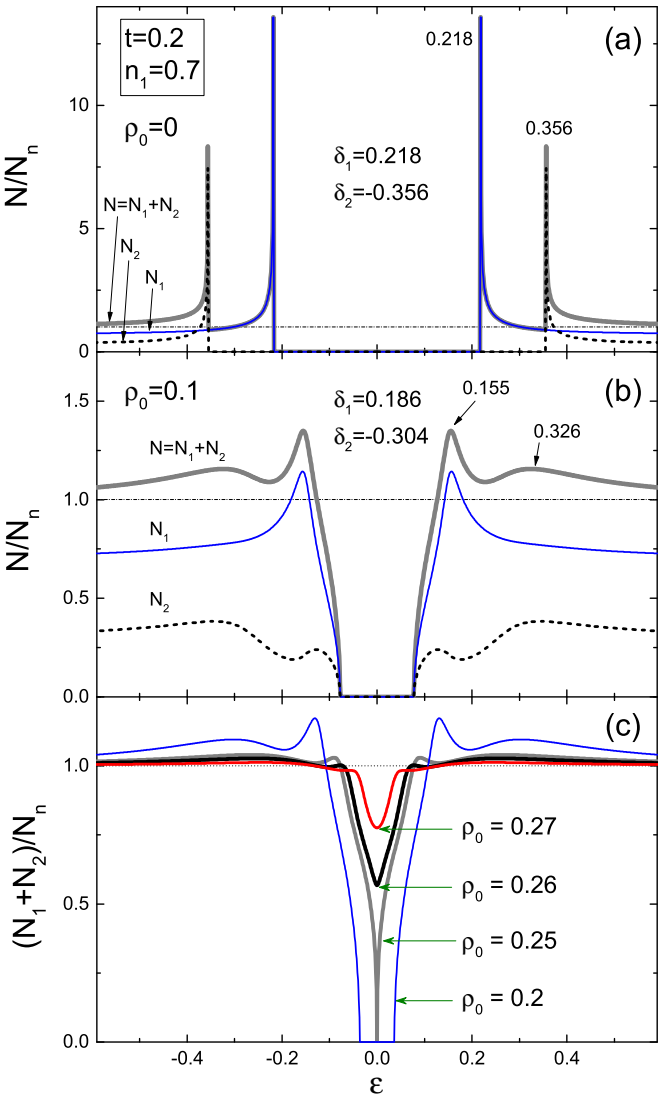

FIG. 4. (a) The clean limit DOS as a function of energy $\varepsilon = \epsilon/2\pi T_{c0}$ for $\lambda = -0.6$ and $n_1 = 0.7$ at $t = 0.2$. (b) The same as (a), but for the interband scattering parameter $\rho_0 = 0.1$. The bands' order parameters for this case are $\delta_1 = 0.186$, $|\delta_2| = 0.304$; $N(\varepsilon)$ has a typical two-band shape, although the two maxima are not exactly positioned at $|\delta_{1,2}|$. (c) The total DOS for a set of scattering parameters ρ_0. Note that with increasing scattering, in the gapless state, the DOS acquires a V shape with a nonzero minimum.

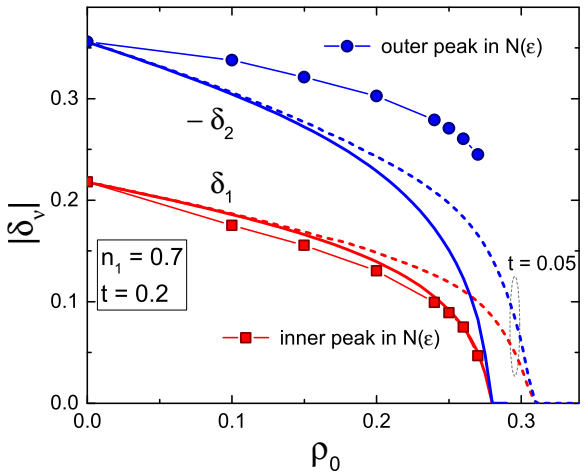

FIG. 5. Peak positions of DOS $N(\varepsilon)$ vs ρ_0 marked as dots along with the bands' order parameters $|\delta_{1,2}|$; solid lines are for $t = 0.2$. The dashed lines are $|\delta_{1,2}|$ for $t = 0.05$.

where the gap does not coincide with the order parameter [27,28].

A remarkable feature of DOS is worth noting: although $\Delta_1 \neq |\Delta_2|$, the calculated energy intervals where $N_\nu(\varepsilon) = 0$ (the energy gaps) are the same for the two bands; see panel (b) of Fig. 4. This was noticed some time ago by Schopohl and Scharnberg who studied the two-band model for superconducting transition metals [4].

In Fig. 5 the positions of DOS $N(\varepsilon)$ maxima are plotted along with the bands' order parameters $|\delta_{1,2}|$ to show that, while the first peak is positioned only slightly under δ_1, the second peak is well above $|\delta_2|$ for all scattering parameters ρ_0. This feature has to be taken into account when, e.g., STM data on $N(\varepsilon)$ are interpreted.

It is worth noting that the energy dependence of DOS $N(\varepsilon)$ in the gapless state, shown in the panel (c) of Fig. 4, has a V shape which should not be confused with a similar shape, e.g., in one-band d-wave materials. Another feature to note is that in the gapless state (in this case $\rho_0 > 0.25$) the two-band signature is hardly seen. This feature is pronounced in Fig. 6

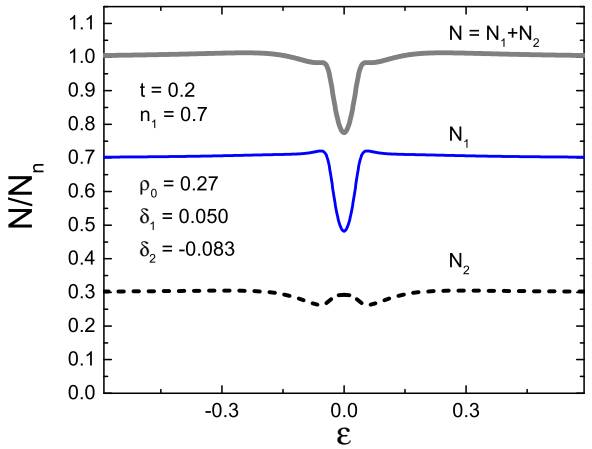

FIG. 6. The density of states N normalized on N_n vs energy ε (in units $2\pi T_{c0}$) for $n_1 = 0.7$, $t = 0.2$ in the gapless state with $\rho_0 = 0.27$.

where both N_1 and N_2 are shown for $n_1 = 0.7$. We also observe that the band with $n_2 = 0.3$ and a larger value of the order parameter ($|\delta_2| = 0.083$) has nearly constant density of states $N_2(\varepsilon)/N_n \approx 0.3$ at all energies, close to the normal state value. This has implications for, e.g., thermal conductivity.

Zero-bias DOS N_0

At zero energy, the system (49) is simplified. Multiply the first equation by n_1, the second by n_2, and add them up: $0 = n_1\delta_1 g_1 + n_2\delta_2 g_2$. Next, substitute $g_2 = -(n_1\delta_1/n_2\delta_2)g_1$ back to the first of Eqs. (49) to obtain for g_1

$$\frac{2\delta_1}{n_2\rho} = \sqrt{1 - \frac{n_1^2\delta_1^2}{n_2^2\delta_2^2}g_1^2} - \frac{n_1\delta_1}{n_2\delta_2}\sqrt{1-g_1^2}. \tag{50}$$

This can be resolved relative to g_1. After simple algebra one obtains the total zero-energy DOS N_0:

$$\frac{N_0}{N_n} = \frac{n_1(\delta_2-\delta_1)}{\delta_2}\mathrm{Re}\sqrt{1 - \frac{\left[\left(n_2^2\delta_2^2 - n_1^2\delta_1^2\right)\rho_0^2 - 4\delta_1^2\delta_2^2\right]^2}{16n_1^2\rho_0^2\delta_1^4\delta_2^2}}. \tag{51}$$

For $n_1 = n_2, \delta_1 = -\delta_2 = \delta$, this reduces to

$$\frac{N_0(\rho_0,T)}{N_n} = \mathrm{Re}\sqrt{1 - \frac{4\delta^2(\rho_0,T)}{\rho_0^2}}. \tag{52}$$

Clearly, the solution of $\tilde\rho = 2|\delta(\tilde\rho)|$ separates the domain $\rho_0 < \tilde\rho$, where $N_0 = 0$ and the superconductivity is gapped, and the gapless region $\tilde\rho < \rho_0 < \rho_c$.

An example of numerically evaluated DOS for $n_1 = 0.5$ at $t = T/T_{c0} = 0.2$ is the left curve of Fig. 7. The lower boundary of the gapless domain, $\tilde\rho \approx 0.236$, is ≈ 0.91 of the critical value 0.26, close to the estimate for this domain at $T = 0$ for magnetic impurities of a single-band isotropic material [27].

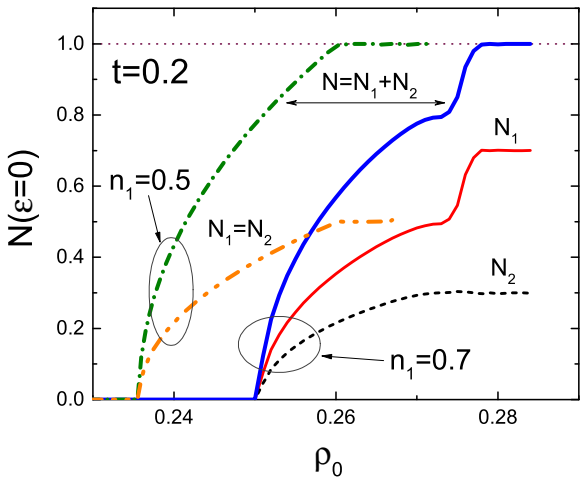

FIG. 7. Left: the zero-bias DOS (normalizeed to N_n) as a function of ρ_0 for $\lambda = -0.6$, $t = 0.2$, and $n_1 = 0.5$; in this case, $\tilde\rho \approx 0.236$ and $\rho_c \approx 0.26$ so that for $0.236 < \rho_0 < 0.26$ the superconductivity is gapless. Right: DOS(ρ_0) at zero energy for the same λ and t, but $n_1 = 0.7$.

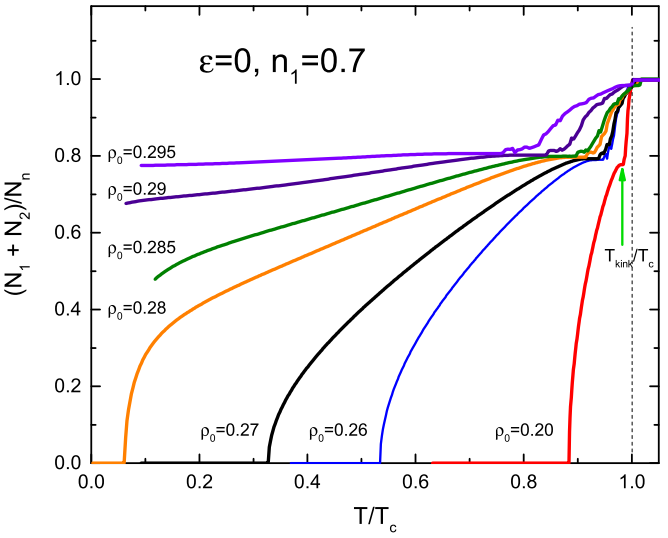

FIG. 8. DOS N_0/N_n at zero energy vs reduced temperature T/T_c for $n_1 = 0.7$ and the set of scattering parameters indicated. Note that the temperature is normalized here on actual T_c, unlike most of the text where T/T_{c0} is used.

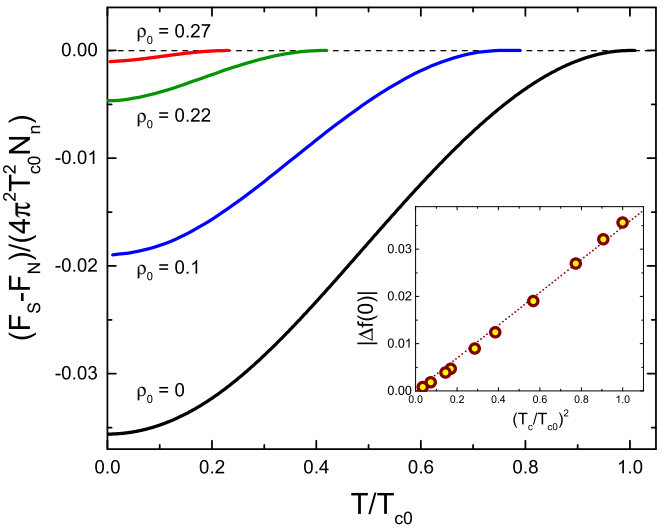

FIG. 9. The temperature dependence of the condensation energy normalized on $4\pi^2 T_{c0}^2 N_n$ for $n_1 = 0.7$ and the set of scattering parameters ρ_0. The inset shows that the normalized condensation energy at $T = 0$ scales approximately as T_c^2.

Similarly one can extract an equation for $\tilde{\rho}$ from Eq. (51) for $n_1 \neq n_2$:

$$\tilde{\rho} = \frac{2\delta_1|\delta_2|}{n_1\delta_1 + n_2|\delta_2|}. \tag{53}$$

An interesting feature of $N_0(\varepsilon)$ seen at the right of Fig. 7 is a sharp drop near $\rho_0 = 0.28$ at which $t = 0.2$ corresponds to the critical temperature. This feature is seen better yet on the plot of N as a function of temperature at fixed ρ_0 in Fig. 8. We observe that the temperature interval of the gapless state near T_c increases with growing ρ_0 and covers all T's when $\rho_0 \to \tilde{\rho}$, with $\tilde{\rho}$ in this case slightly larger than 0.28. Another feature worth noting is a fast drop of zero-bias N_0 near T_c, the nature of which at this stage is not clear.

F. Energy and specific heat

Substituting the self-consistency Eqs. (12) in the functional (13) one obtains

$$\frac{\Omega}{N_n} = -2\pi T \sum_{\nu,\omega} n_\nu[\Delta_\nu f_\nu + 2\omega(g_\nu - 1)] - 2\pi T \frac{n_1 n_2}{\tau} \sum_{\omega} (f_1 f_2 + g_1 g_2 - 1). \tag{54}$$

We normalize $\Omega(T)/N_n$ on $4\pi^2 T_{c0}^2$:

$$\frac{F_n - F_s}{4\pi^2 T_{c0}^2 N_n} = t \sum_{\nu,l} n_\nu[\delta_\nu f_\nu + t(2l+1)(g_\nu - 1)] + t\, n_1 n_2 \rho_{12} \sum_{l} (f_1 f_2 + g_1 g_2 - 1). \tag{55}$$

Since we can calculate δ_ν and f_ν at a given temperature, it is an easy task to evaluate the condensation energy; see Fig. 9. The inset in this figure shows that the normalized condensation energy at $T = 0$ scales approximately as T_c^2, a nearly universal property of all superconductors [29,30].

Having the condensation energy, one finds the thermodynamic critical field $H_c = \sqrt{8\pi(F_N - F_S)}$. We normalize it to the zero-T value $H_c^{(0)} = \sqrt{4\pi N(0)}\Delta_0(0)$ for the clean case and $n_1 = n_2$ to get

$$h_c(t) = \frac{H_c(t)}{H_c^{(0)}} = 2\sqrt{2}\, e^{\gamma}\sqrt{\Phi(t)}, \tag{56}$$

where $\Phi(t)$ is the right-hand side of Eq. (55). With this normalization, the clean limit $h_c(0) = 1$ for $n_1 = n_2$. Figure 10 shows numerical results for parameters indicated.

The specific heat can now be evaluated for fixed n_1 and ρ_0. An example is shown in the upper panel of Fig. 11. The lower panel of Fig. 11 shows the specific heat vs reduced temperature for a few n_1 of clean materials. Note that the jump at T_c in this case is given in Eq. (30) as a function of n_1, n_2. On the other hand, $T_{c0}(n_1)$ is given in Eq. (21) which allows one to evaluate

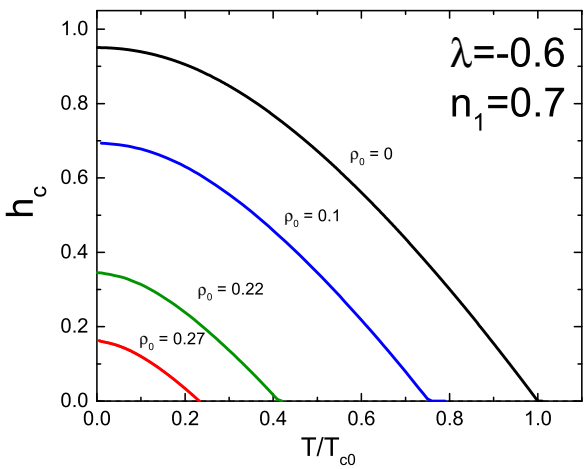

FIG. 10. The thermodynamic critical field $h_c(t) = H_c/H_{c0}$ for $n_1 = 0.7$ and $\lambda = -0.6$.

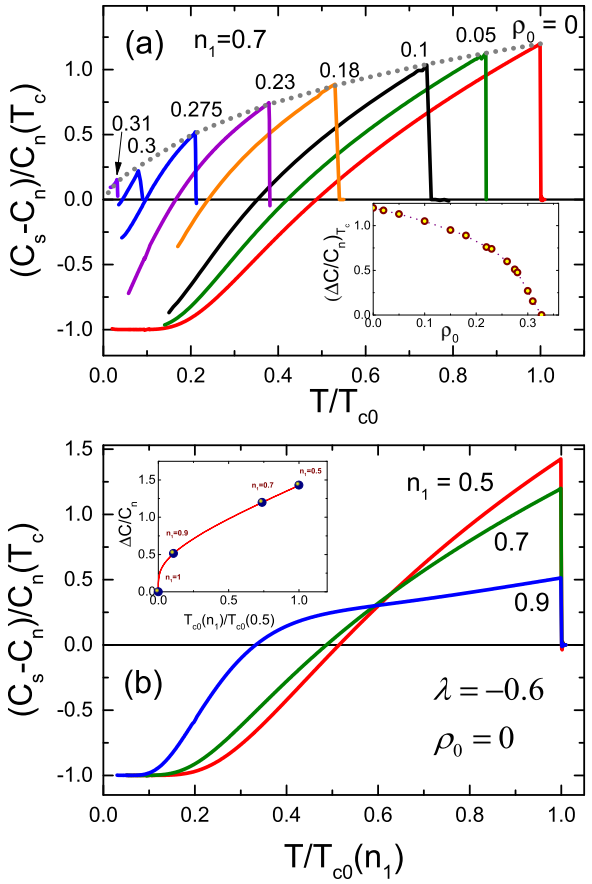

FIG. 11. Top: the specific heat vs $T/T_{c0}(0.7)$ for a few scattering parameters ρ_0. Bottom: the specific heat vs $T/T_{c0}(n_1)$ for $n_1 = 0.5$, 0.7, and 0.9. Inset: the specific heat jump at the critical temperature calculated numerically (dots) and according to Eq. (57) (solid line).

the jump $\Delta C/C_n$ as a function of T_{c0}:

$$\left.\frac{\Delta C}{C_n}\right|_{T_c} = \frac{48}{7\zeta(3)\lambda^2}\left(\ln\frac{T_{c0}(n_1)}{T_{c0}(0.5)} - \frac{2}{|\lambda|}\right)^{-2}. \tag{57}$$

The inset in the lower panel shows this dependence. For $n_1 = n_2$, analytic evaluation of the specific heat jump is done in Appendix B for any scattering rate.

G. Penetration depth

If the ground state functions (called $f^{(0)}$, $g^{(0)}$ in this section) are known, one can study perturbations of the uniform state by a weak magnetic field; i.e., the problem of the London penetration depth. The perturbations, $f^{(1)}$, $g^{(1)}$, are found from Eqs. (1) and (2) which include gradient terms and magnetic field. We have for the first band [16]

$$\boldsymbol{v}_1\boldsymbol{\Pi} f_1 = 2\Delta_1 g_1 - 2\omega f_1 + \frac{n_1}{\tau_{11}}[g_1\langle f\rangle_1 - f_1\langle g\rangle_1] + \frac{n_2}{\tau_{12}}[g_1\langle f\rangle_2 - f_1\langle g\rangle_2]. \tag{58}$$

The second equation is obtained by $1 \leftrightarrow 2$. Two equations for $f^+_{1,2}$ are obtained from these by complex conjugation and by $\boldsymbol{v} \to -\boldsymbol{v}$ [15]. Normalizations $g_\nu^2 + f_\nu f_\nu^+ = 1$ complete the system.

We now note that the London approximation suffices for the problem of weak field penetration. In this approximation only the overall macroscopic phase θ depends on coordinates whereas the order parameter modulus remains unperturbed. We thus replace $\Delta \to \Delta e^{i\theta(\boldsymbol{r})}$ and look for solutions in the form

$$f_\nu = \left(f_\nu^{(0)} + f_\nu^{(1)}\right)e^{i\theta(\boldsymbol{r})}, \quad f_\nu^+ = \left(f_\nu^{(0)} + f_\nu^{(1)+}\right)e^{-i\theta(\boldsymbol{r})},$$
$$g_\nu = g_\nu^{(0)} + g_\nu^{(1)}, \quad \nu = 1,2. \tag{59}$$

Note that the first corrections $f_\nu^{(1)}$, $g_\nu^{(1)}$ depend on $\boldsymbol{k}$ (or $\boldsymbol{v}$) in the form $\boldsymbol{vP}$ with $\boldsymbol{P} = \nabla\theta + 2\pi\boldsymbol{A}/\phi_0$, so that their Fermi surface averages vanish (unless the material does not have inversion symmetry, the case we do not consider).

We obtain for the corrections in the first band

$$g_1^{(1)}\Delta_1' - f_1^{(1)}\omega_1' = if_1^{(0)}\boldsymbol{v}_1\boldsymbol{P}/2,$$
$$g_1^{(0)}g_1^{(1)} + f_1^{(0)}f_1^{(1)} = 0, \tag{60}$$

where

$$\Delta_1' = \Delta_1 + n_1 f_1^{(0)}/2\tau_{11} + n_2 f_2^{(0)}/2\tau_{12}, \tag{61}$$

$$\omega_1' = \omega + n_1 g_1^{(0)}/2\tau_{11} + n_2 g_2^{(0)}/2\tau_{12} \tag{62}$$

contain only the unperturbed $f^{(0)}$, $g^{(0)}$. System (60) yields [31]

$$g_1^{(1)} = \frac{if_1^{(0)2}\,\boldsymbol{v}_1\boldsymbol{P}}{2\left(\Delta_1' f_1^{(0)} + \omega_1' g_1^{(0)}\right)} = i\,\frac{f_1^{(0)2}g_1^{(0)}}{2\omega_1'}\,\boldsymbol{v}_1\boldsymbol{P}. \tag{63}$$

The correction $g_2^{(1)}$ is obtained by the replacement $1 \to 2$.

To evaluate the penetration depth we turn to the Eilenberger expression for the current density [15],

$$\boldsymbol{j} = -4\pi|e|N_n T\,\mathrm{Im}\sum_{\omega>0}\langle\boldsymbol{v}g\rangle, \tag{64}$$

where $\langle\boldsymbol{v}g\rangle = \langle\boldsymbol{v}g^{(1)}\rangle$ since $\langle\boldsymbol{v}g^{(0)}\rangle = 0$. Substitute here $g_\nu^{(1)}$ of Eq. (63) and compare with the London relation

$$\frac{4\pi}{c}j_i = -(\lambda^2)_{ik}^{-1}\left(\frac{\phi_0}{2\pi}\nabla\theta + \boldsymbol{A}\right)_k. \tag{65}$$

Here, $(\lambda^2)_{ik}^{-1}$ is the tensor of the inverse squared penetration depth; summation over k is implied. Hence, the in-plane component of this tensor is

$$\lambda_{xx}^{-2} = \frac{16\pi^2 e^2 N_n T}{c^2}\sum_{\nu,\omega} n_\nu\langle v_x^2\rangle_\nu \frac{f_\nu^2 g_\nu}{\omega_\nu'}. \tag{66}$$

Only the unperturbed functions $f^{(0)}$, $g^{(0)}$ enter the penetration depth; for brevity we dropped superscripts (0). Since we know how to evaluate f's at each temperature, the evaluation of the London penetration depth is straightforward.

For numerical work we normalize $\lambda_{xx}^{-2}(T,\rho_0)$ on the zero-T value for clean bands:

$$\lambda_{xx}^{-2}(0,0) = \frac{8\pi e^2 N_n}{c^2}\langle v_x^2\rangle = \frac{8\pi e^2 N_n}{c^2}\sum_\nu n_\nu\langle v_x^2\rangle_\nu. \tag{67}$$

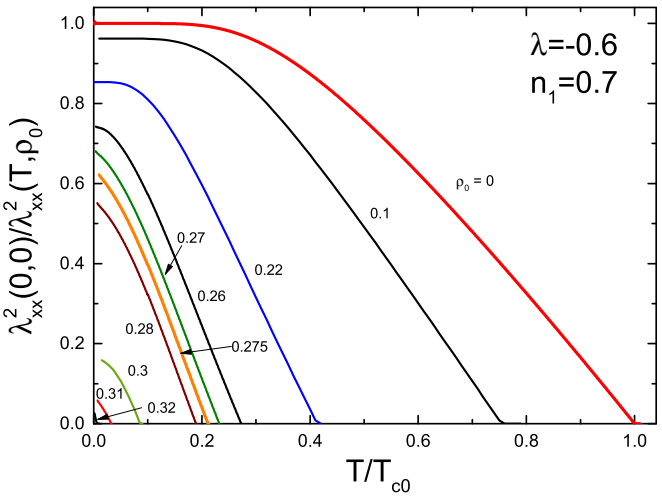

FIG. 12. The inverse square of the in-plane penetration depth normalized on the zero-T clean limit value vs $t = T/T_{c0}$ for a set of scattering parameters ρ_0. In this calculation $\langle v_x^2\rangle_1/\langle v_x^2\rangle_2 = 1$ and the intraband $\rho_{11} = \rho_{22} = 0$.

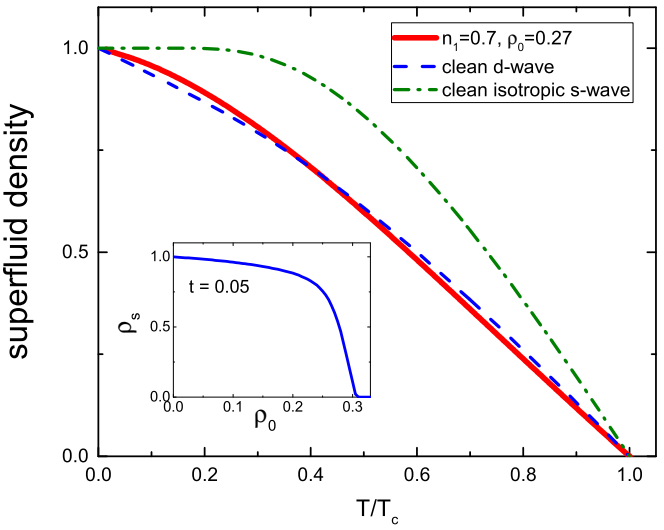

FIG. 13. The superfluid density ρ_s vs $t = T/T_{c0}$ for $n_1 = 0.7$ and $\rho_0 = 0.27$ of the gapless state normalized on the value at $T = 0$. Superfluid densities for s- and d-wave clean cases are shown for comparison.

Hence, we have for the dimensionless penetration depth

$$\Lambda_{xx}^{-2} = \frac{\lambda_{xx}^{-2}(T,\rho_0)}{\lambda_{xx}^{-2}(0,0)} = \frac{\sum_{\nu,\omega} n_\nu \langle v_x^2\rangle_\nu f_\nu^2 g_\nu/\eta_\nu}{\sum_\nu n_\nu \langle v_x^2\rangle_\nu}, \tag{68}$$

$$\eta_\nu = l + \frac{1}{2} + \frac{n_\nu g_\nu \rho_{\nu\nu}}{2t} + \frac{n_{\bar\nu} g_{\bar\nu} \rho_{12}}{2t}, \quad \rho_{\mu\nu} = \frac{\hbar}{2\pi T_{c0}\tau_{\mu\nu}}. \tag{69}$$

Here, $g_\nu = \sqrt{1 - f_\nu^2}$; $\bar\nu$ denotes the value other than ν; in fact, Λ^{-2} depends only on the ratio of averaged Fermi velocities.

Numerically evaluated $\Lambda_{xx}^{-2}(t)$ is shown in Fig. 12 for the scattering parameters indicated. In this particular calculation $\rho_{11} = \rho_{22} = 0$; incorporating the intraband scattering does not change qualitatively the behavior of the superfluid density with respect to interband scattering and will be presented elsewhere.

We note that for a weak interband scattering the low temperature superfluid density (SFD) is nearly T independent, as expected for gapped materials. With increasing interband scattering, the flat domain of SFD shrinks and disappears altogether in the gapless state starting roughly with $\rho_0 \approx 0.27$. Remarkably, in the gapless state SFD becomes close to linear, the behavior commonly ascribed to the order parameter nodes. To show that the latter interpretation can be misleading, we plot SFD for $\rho_0 = 0.27$ along with the known result for the d-wave materials in Fig. 13.

V. DISCUSSION

Many Fe-based compounds are thought to have $\pm s$ symmetry of the order parameter. By considering a model with the interband coupling $\lambda_{12} < 0$ (repulsion) we assure that the bands' order parameters Δ_1 and Δ_2 have opposite signs.

Using the quasiclassical approach, we formulate equations governing two-band systems with exclusively interband coupling and interband scattering. To describe thermodynamic properties we construct the energy functional, minimization of which gives the two-band Eilenberger equations along with the self-consistency equations. This allows us to evaluate the condensation energy along with the specific heat and, in particular, the specific heat jump at T_c.

Except for some limiting cases which are dealt with analytically, we resort to numerical solutions which have the advantage of being straightforward, especially when the analytic approach is too cumbersome if at all possible. For completeness we reproduce some of the known results within our approach.

We focus on properties which are affected by the pair-breaking character of the interband scattering. The question of pair breaking in Fe-based materials has been raised in the past, basically on the basis of work by Abrikosov and Gor'kov on magnetic impurities; see, e.g., Refs. [26,32]. However, the source of the pair-breaking was not specified, so that this approach was not generally accepted. Still, it seemed to describe a number of observed properties such as the power-law low temperature dependence of the superfluid density [33] or the experimentally observed scaling of the specific heat jump $\Delta C \propto T_c^3$ [34].

Interband scattering by nonmagnetic disorder has qualitatively similar pair-breaking features. In fact, for two bands with equal DOS, the T_c suppression is described by the Abrikosov-Gor'kov equation (35) for a one-band d-wave material. By evaluating the energy dependence of the density of states, we show that sufficiently strong nonmagnetic interband scattering results in a gapless state, and we determine the range of scattering parameters where this state emerges.

The presence of two bands, however, brings in an extra feature: the critical temperature is suppressed not only by the interband scattering but also by a mismatch of bands' DOS n_1 and n_2. The T_c dependence on n_1 has a domelike shape of Fig. 1, which suggests that the ubiquitous domes $T_c(x)$ at phase diagrams of, e.g., Fe-based compounds (x is the doping variable) could be related to changes with x of the DOS mismatch of bands involved.

It is worth noting that the strong pair breaking regime when $T_c \to 0$ in a two-band system with nonmagnetic interband scattering differs from the strong spin-flip scattering by magnetic impurities. The point is that the latter is always complicated by possibility of moments ordering or by glassy and Kondo phenomena, which are clearly absent for the nonmagnetic interband scattering.

Properties of the gapless state in the two-band case are richer than in the one-band Abrikosov-Gor'kov situation. Particularly interesting are properties of DOS in the gapless state. We show that whereas the energy dependence $N_1(\varepsilon)$ of the "major" band with larger normal state DOS n_1 has the ubiquitous V shape, the DOS on the "minor" band is close to being normal. This suggests a high heat conductance often seen in Fe-based compounds.

Turning to our results on effects of the interband scattering upon the penetration depth, it is instructive to recall the experimental situation. What is commonly measured with high accuracy are changes in the London penetration depth, $\Delta\lambda(T) \equiv \lambda(T) - \lambda(0)$. At low temperatures, these are related to the superfluid density $\rho_s \equiv \lambda(0)^2/\lambda(T)^2 \approx 1 - 2\Delta\lambda/\lambda(0)$. It is convenient to analyze low-temperature behavior as $\Delta\lambda(T) \approx AT^n$. According to conventional picture, the line nodes of the order parameter result in a linear behavior, $n = 1$, whereas fully gapped order parameters (e.g., s_{++} or $s_{\pm}$) give nearly flat exponential variation, which in practice is indistinguishable from $n > 3$.

In the presence of symmetry-imposed line nodes (e.g., d wave), intensifying scattering causes monotonic increase of the exponent from $n = 1$ to $n = 2$ [35–38], whereas in the conventional s wave (including multiband s_{++}) the low temperature SFD $\rho_s(T)$ remains exponentially flat (whereas T_c does not change).

However, we show in this work that for fully gapped $\pm s$ pairing, where potential interband scattering is pair breaking, the superfluid density evolves from exponentially flat to nearly linear as shown in Figs. 12 and 13. The corresponding exponents in power-law fits would change from $n > 3$ to well below $n = 2$. In fact, for a strong T_c suppression, in the gapless regime, the entire curve of $\rho_s(T)$ is surprisingly close to a clean d-wave dependence; see Fig. 13. Thus, in principle, one can change the s-wave-like to the d-wave-like behavior of $\rho_s(T)$ just by introducing disorder, resulting in a change of the interband scattering. Interesting enough, such a behavior has been seen in $BaFe_2As_2$ doped with Co or Ni: the exponent n decreased after irradiation [39].

ACKNOWLEDGMENTS

Discussions with A. Gurevich, V. Mishra and A. Chubukov are gratefully appreciated. We thank Joerg Schmalian who turned our attention to the question of how T_c changes when approaching critical values of the scattering rate and of DOS n_1 (Sec. IV B). This work was supported by the U.S. Department of Energy (DOE), Office of Science, Basic Energy Sciences, Materials Science and Engineering Division. Ames Laboratory is operated for the U.S. DOE by Iowa State University under contract DE-AC02-07CH11358.

APPENDIX A: SELF-CONSISTENCY EQUATIONS

Consider the first of the self-consistency equations (12):

$$-\frac{\Delta_1}{|\lambda|n_2} = 2\pi T \sum_{\omega}^{\omega_D} f_2. \tag{A1}$$

Add and subtract to the right-hand side $2\pi T \sum_{\omega}^{\omega_D}(\Delta_2/\omega)$ to have

$$2\pi T \sum_{\omega}^{\omega_D} \frac{\Delta_2}{\omega} - 2\pi T \sum_{\omega}^{\infty} \left(\frac{\Delta_2}{\omega} - f_2\right). \tag{A2}$$

In the second convergent sum, ω_D is replaced with ∞, whereas for the first sum use the identity

$$2\pi T \sum_{\omega}^{\omega_D} \frac{1}{\omega} = \frac{1}{\tilde{\lambda}} - \ln\frac{T}{T_{c0}}, \quad \tilde{\lambda} = |\lambda|\sqrt{n_1 n_2}. \tag{A3}$$

We then obtain

$$\Delta_2 \ln\frac{T_{c0}}{T} + \frac{\sqrt{n_1}\Delta_1 + \sqrt{n_2}\Delta_2}{\tilde{\lambda}\sqrt{n_2}} = 2\pi T \sum_{\omega}^{\infty} \left(\frac{\Delta_2}{\omega} - f_2\right). \tag{A4}$$

APPENDIX B: THE CASE $n_1 = n_2$

In this case $\Delta_1 = -\Delta_2 = \Delta$, $f_1 = -f_2 = f$, and $g_2 = g_1 = g$. Examine first the situation near T_c:

$$f = \frac{\Delta}{\omega'} - \frac{\Delta^3}{2\omega'^3}, \quad g = 1 - \frac{\Delta^2}{2\omega'^2} + \frac{3\Delta^4}{8\omega'^4}. \tag{B1}$$

The self-consistency condition for this situation is

$$\Delta/\lambda = -\pi T \sum_{\omega}^{\omega_D} f. \tag{B2}$$

Substituting here f of Eq. (B1), one has

$$\Delta = -\frac{\lambda}{2}\left(A\Delta - \frac{D}{2}\Delta^3\right), \tag{B3}$$

with

$$A = \sum_{0}^{\omega_D} \frac{2\pi T}{\omega'} = \ln\frac{\omega_D}{2\pi T} - \psi\left(\frac{\rho+1}{2}\right),$$
$$D = \sum_{0}^{\infty} \frac{2\pi T_c}{\omega_c'^3} = -\frac{1}{8\pi^2 T_c^2}\psi''\left(\frac{\rho_c+1}{2}\right). \tag{B4}$$

Here, $\rho_c = 1/2\pi T_c\tau$. Near T_c, only terms of order not smaller than $(\delta t)^{3/2}$ should be retained. Since $\Delta \propto (\delta t)^{1/2}$, one can set $T = T_c$ in the coefficient D. Hence, one obtains

$$\Delta^2 = \frac{2}{D}\left(A + \frac{2}{\lambda}\right). \tag{B5}$$

We now transform the logartihmic term in A:

$$\ln\frac{\omega_D}{2\pi T} = \ln\frac{\omega_D}{2\pi T_{c0}} + \ln\frac{T_{c0}}{T_c} + \ln\frac{T_c}{T}$$
$$= \psi\left(\frac{1}{2}\right) + \frac{1}{\tilde{\lambda}} + \ln\frac{T_{c0}}{T_c} + \delta t, \tag{B6}$$

where the definition of T_{c0}, $\ln(2\omega_D e^{\gamma}/\pi T_{c0}) = 2/|\lambda|$, has been used. Next, we expand the psi-function term in A,

$$\psi\left(\frac{\rho+1}{2}\right) = \psi\left(\frac{\rho_c+1}{2}\right) + \frac{\rho_c}{2}\psi'\left(\frac{\rho_c+1}{2}\right)\delta t. \quad \text{(B7)}$$

Finally, using Eq. (35) for T_c, we obtain

$$\Delta^2 = -\frac{16\pi^2 T_c^2}{\psi''}\left(1 - \frac{\rho_c}{2}\psi'\right)\delta t, \quad \text{(B8)}$$

where psi functions are taken at $(\rho_c + 1)/2$.

Now we turn to the functional (13):

$$\frac{\Omega}{N_n} = -\frac{2\Delta^2}{\lambda} - 2\pi T \sum_{\omega}\left\{2[\Delta f + \omega(g-1)] - \frac{f^2}{2\tau}\right\}. \quad \text{(B9)}$$

Substituting here f of Eq. (B1) and Δ of Eq. (B8) we obtain after straightforward algebra

$$\frac{F_s - F_s}{N_n} = \frac{4\pi^2 T_c^2}{\psi''}\left(2 - \frac{\rho_c\psi'''}{3\psi''}\right)\left(1 - \frac{\rho_c}{2}\psi'\right)^2(\delta t)^2, \quad \text{(B10)}$$

where the psi functions are taken at $(\rho_c + 1)/2$. The specific heat jump follows:

$$\frac{C_s - C_n}{C_n}\Big|_{T_c} = -\frac{24}{\psi''}\left(1 - \frac{\rho_c\psi'''}{6\psi''}\right)\left(1 - \frac{\rho_c\psi'}{2}\right)^2. \quad \text{(B11)}$$

In the clean limit, this gives $12/7\zeta(3) = 1.43$. Since T_c can be evaluated for each ρ_c, one can plot the jump vs T_c/T_{c0}, Fig. 11(b).

In fact, this behavior of $\Delta C/C_n(T_c)$ is qualitatively similar to the one-band d wave (although there the clean limit value is 2/3 of 1.43). One can associate this similarity to the fact that in both cases $\langle\Delta\rangle = 0$.

[1] C. C. Sung and V. K. Wong, J. Phys. Chem. Solids **28**, 1933 (1967).
[2] W. S. Chow, Phys. Rev. **172**, 467 (1968).
[3] V. A. Moskalenko, A. M. Ursu, and N. I. Botoshan, Phys. Lett. A **44**, 183 (1973).
[4] N. Schopohl and K. Scharnberg, Solid State Commun. **22**, 371 (1977).
[5] A. A. Golubov and I. I. Mazin, Phys. Rev. B **55**, 15146 (1997).
[6] D. V. Efremov, M. M. Korshunov, O. V. Dolgov, A. A. Golubov, and P. J. Hirschfeld, Phys. Rev. B **84**, 180512(R) (2011).
[7] A. B. Vorontsov, M. G. Vavilov, and A. V. Chubukov, Phys. Rev. B **79**, 140507(R) (2009).
[8] O. V. Dolgov, A. A. Golubov, and D Parker, New J. Phys. **11**, 075012 (2009).
[9] D. V. Efremov, A. A. Golubov, and O. V. Dolgov, New J. Phys. **15**, 013002 (2013).
[10] P. J. Hirschfeld, M. M. Korshunov, and I. I. Mazin, Rep. Prog. Phys. **74**, 124508 (2011)
[11] I. I. Mazin and J. Schmalian, Physica C: Supercond. **469**, 614 (1995).
[12] M. Hoyer, S. V. Syzranov, and J. Schmalian, Phys. Rev. B **89**, 214504 (2014).
[13] M. Hoyer, M. S. Scheurer, S. V. Syzranov, and J. Schmalian, Phys. Rev. B **91**, 054501 (2015).
[14] M. M. Korshunov, Yu. N. Togushova, and O. V. Dolgov, J. Supercond. Nov. Magn. **29**, 1089 (2016).
[15] G. Eilenberger, Z. Phys. **214**, 195 (1968).
[16] V. G. Kogan and N. V. Zhelezina, Phys. Rev. B **69**, 132506 (2004).
[17] V. G. Kogan, C. Martin, and R. Prozorov, Phys. Rev. B **80**, 014507 (2009).
[18] B. T. Geilikman, Usp. Fiz. Nauk **88**, 327 (1966).
[19] V. A. Moskalenko, Phys. Met. Metallogr. **8**, 503 (1959).
[20] B. T. Geilikman, R. O. Zaitsev, and V. Z. Kresin, Sov. Phys. Solid State **9**, 642 (1967).
[21] Y. Bang and G. R. Stewart, New J. Phys. **18**, 023017 (2016).
[22] This is a feature of the exclusively interband coupling. For nonzero λ_{11} and λ_{22}, the ratio of order parameters depends on couplings along with DOS. L. Gor'kov, Phys. Rev. B **86**, 060501(R) (2012).
[23] V. G. Kogan and J. Schmalian, Phys. Rev. B **83**, 054515 (2011).
[24] V. A. Moskalenko, M. E. Palistrant, and V. M. Vakalyuk, Sov. Phys. Usp. **161**, 155 (1991).
[25] L. A. Openov, Phys. Rev. B **58**, 9468 (1998).
[26] V. G. Kogan, Phys. Rev. B **81**, 184528 (2010).
[27] A. A. Abrikosov and L. P. Gor'kov, Zh. Eksp. Teor. Fiz. **39**, 1781 (1060) [Sov. Phys. JETP **12**, 1243 (1961)].
[28] K. Maki, in *Superconductivity*, Vol. 2, edited by R. D. Parks (Marcel Dekker, New York, 1969).
[29] J. P. Carbotte, Rev. Mod. Phys. **62**, 1027 (1990).
[30] J. S. Kim, G. N. Tam, and G. R. Stewart, Phys. Rev. B **92**, 224509 (2015).
[31] To justify the last step consider $g_1(\Delta' f_1^{(0)} + \omega' g_1^{(0)}) = g_1^{(0)}\Delta' f_1^{(0)} + \omega'(1 - f_1^{(0)2}) = \omega'$ since $\Delta' g_1^{(0)} - \omega' f_1^{(0)} = 0$ is the equilibrium Eilenberger equation.
[32] V. G. Kogan, Phys. Rev. B **80**, 214532 (2009).
[33] R. T. Gordon, H. Kim, N. Salovich, R. W. Giannetta, R. M. Fernandes, V. G. Kogan, T. Prozorov, S. L. Bud'ko, P. C. Canfield, M. A. Tanatar, and R. Prozorov, Phys. Rev. B **82**, 054507 (2010).
[34] S. L. Bud'ko, Ni Ni, and P. C. Canfield, Phys. Rev. B **79**, 220516(R) (2009).
[35] Y. Noat, T. Cren, V. Dubost, S. Lange, F. Debontridder, P. Toulemonde, J. Marcus, A. Sulpice, W. Sacks, and D. Roditchev, J. Phys.: Condens. Matter **22**, 465701 (2010).
[36] L. Y. L. Shen, N. M. Senozan, and N. E. Phillips, Phys. Rev. Lett. **14**, 1025 (1965).
[37] P. J. Hirschfeld and N. Goldenfeld, Phys. Rev. B **48**, 4219 (1993).
[38] V. G. Kogan, R. Prozorov, and V. Mishra, Phys. Rev. B **88**, 224508 (2013).
[39] H. Kim, R. T. Gordon, M. A. Tanatar, J. Hua, U. Welp, W. K. Kwok, N. Ni, S. L. Bud'ko, P. C. Canfield, A. B. Vorontsov, and R. Prozorov, Phys. Rev. B **82**, 060518 (2010).